Development 134, 3713-3722 (2007) doi:10.1242/dev.02873

Cell tracing reveals a dorsoventral lineage restriction plane in the mouse limb bud mesenchyme

Carlos G. Arques[1], Roisin Doohan[1], James Sharpe[2] and Miguel Torres[1,*]

Regionalization of embryonic fields into independent units of growth and patterning is a widespread strategy during metazoan development. Compartments represent a particular instance of this regionalization, in which unit coherence is maintained by cell lineage restriction between adjacent regions. Lineage compartments have been described during insect and vertebrate development. Two common characteristics of the compartments described so far are their occurrence in epithelial structures and the presence of signaling regions at compartment borders. Whereas *Drosophila* compartmental organization represents a background subdivision of embryonic fields that is not necessarily related to anatomical structures, vertebrate compartment borders described thus far coincide with, or anticipate, anatomical or cell-type discontinuities. Here, we describe a general method for clonal analysis in the mouse and use it to determine the topology of clone distribution along the three limb axes. We identify a lineage restriction boundary at the limb mesenchyme dorsoventral border that is unrelated to any anatomical discontinuity, and whose lineage restriction border is not obviously associated with any signaling center. This restriction is the first example in vertebrates of a mechanism of primordium subdivision unrelated to anatomical boundaries. Furthermore, this is the first lineage compartment described within a mesenchymal structure in any organism, suggesting that lineage restrictions are fundamental not only for epithelial structures, but also for mesenchymal field patterning. No lineage compartmentalization was found along the proximodistal or anteroposterior axes, indicating that patterning along these axes does not involve restriction of cell dispersion at specific axial positions.

KEY WORDS: Clonal analysis, Fate maps, Vertebrate limb, Lineage compartments, Lmx1b

INTRODUCTION

Patterning of embryonic primordia involves tight regulation of cell behavior during tissue growth, morphogenesis, lineage diversification and differentiation. Understanding how complex organs develop therefore requires the deciphering of how a cell's behavior is defined by its lineage history, the external cues it senses and its position within the developing primordium. A key feature underlying organ patterning during development is the subdivision of developmental fields into independent units of growth and patterning known as compartments. Compartments were originally described in *Drosophila* imaginal discs as subdivisions (normally hemisections) of organ primordia occurring on an otherwise homogeneous epithelial cell field and whose coherence is maintained by cell lineage (Garcia-Bellido et al., 1973; Lawrence, 1973; Morata and Lawrence, 1975). Compartment boundaries are therefore unique lines at stereotyped positions in a developing organ, across which cell intermingling does not take place, even though it is allowed elsewhere in the primordium. *Drosophila* compartment borders do not necessarily coincide with or anticipate any morphological or cell-type discontinuity even after overt differentiation (reviewed by Blair, 2003). Thus, *Drosophila* compartmental organization is a background subdivision of embryonic fields that serves to establish positional references in the primordium and is not necessarily related to anatomical boundaries in the organism.

[1]Departamento de Biología del Desarrollo Cardiovascular, Centro Nacional de Investigaciones Cardiovasculares, Instituto de Salud Carlos III, E-28029 Madrid, Spain. [2]Center for Genomic Regulation (CRG), Program on Systems Biology, Barcelona, Spain.

*Author for correspondence (e-mail: mtorres@cnic.es)

Accepted 25 May 2007

Lineage restriction units resembling *Drosophila* compartments have also been described in vertebrates. Pioneering work in the chick, involving labeling of multiple neuroepithelial cells with a lipophilic dye, identified cell lineage restriction boundaries at the frontiers between rhombomeres (Fraser et al., 1990). Similarly, fate mapping of multiple cells identified a cell lineage restriction border at the dorsoventral (D-V) boundary of the chick limb ectoderm (Altabef et al., 1997). In the mouse, the use of inducible site-specific recombination (Brocard et al., 1997) has allowed the prospective lineage analysis of groups of cells defined by the expression of particular genes/enhancers (Kimmel et al., 2000). These approaches, collectively known as genetic inducible fate mapping (GIFM), have been used extensively in the analysis of nervous system development, providing insightful information on neural tube regionalization, brain morphogenesis, neural cell-type specification mechanisms and neural stem cell dynamics (reviewed by Joyner and Zervas, 2006). The use of GIFM in the mouse has also identified several other lineage restriction borders in the vertebrate neuroepithelium, such as the midbrain-hindbrain boundary (MHB), the zona limitans intrathalamica (ZLI) and others (reviewed by Kiecker and Lumsden, 2005). Similarly, GIFM has revealed the lineage compartmentalization of the mouse limb ectoderm into dorsal, dorsal apical ectodermal ridge (AER) and ventral compartments (Kimmel et al., 2000).

A common characteristic of the lineage compartments described so far in insects and vertebrates is their occurrence in epithelial structures, so that each compartment is a two-dimensional epithelial area and the compartment border is a line between two adjacent compartments (reviewed by Blair, 2003; Kiecker and Lumsden, 2005; Vincent, 1998). Furthermore, most lineage restriction borders described in both vertebrates and insects are associated with signaling centers (Kiecker and Lumsden, 2005), which suggests that a major role of lineage compartments during embryonic development is signaling-center stabilization.

In contrast to *Drosophila* compartments, however, all lineage restrictions described so far in vertebrates coincide with, or anticipate, anatomical or cell-type discontinuities. The known restrictions in vertebrates may thus not be a background subdivision of embryonic fields, but might instead largely correlate with strategies to allocate cells fated to different anatomical structures. Systematic searches for cell lineage restrictions during vertebrate embryonic development, however, have been limited, and therefore our knowledge of the complete set of restrictions that occur is likely to be incomplete. Efforts in this direction have made use of the low-frequency spontaneous recombination of a mutant *lacZ* transgene (*laacZ*) (Bonnerot and Nicolas, 1993). This transgene, driven either by ubiquitous or specific promoters, has been successfully used to determine fundamental parameters of tissue growth dynamics and regionalization in the developing heart (Meilhac et al., 2004; Meilhac et al., 2003), paraxial mesoderm (Nicolas et al., 1996) and CNS (Mathis and Nicolas, 2000; Mathis et al., 1999; Wilkie et al., 2004). This method is constrained, however, by the inability to control the timing and frequency of recombination events. More recently, GIFM at low recombination frequency has been successfully used in a random retrospective analysis of cell lineage at clonal resolution in the hair follicle (Legue and Nicolas, 2005).

Here, we apply a novel strategy based exclusively on knock-in alleles of ubiquitous expression, which allows unrestricted clonal analysis of cell lineage from the two-cell stage to the adult mouse. Using this strategy, we have analyzed the topology of cell clone distribution in the developing vertebrate limb, with a particular focus on the mesenchyme. The lineage analysis we present demonstrates that there is no lineage compartmentalization at any position along the proximodistal (P-D) or anteroposterior (A-P) axes, indicating that patterning along these axes does not involve restrictions of cell dispersion at specific axial positions. By contrast, we have identified a D-V lineage restriction boundary in the limb mesenchyme. This is the first example from any organism of a lineage boundary restriction operating within a mesenchymal tissue. The resulting D-V lineage compartments are three-dimensional and the compartment border is a plane that is neither associated with any obvious signaling function nor coincident with any anatomical or cell-type discontinuity.

MATERIALS AND METHODS

Mouse strains

RERT and *R26R* or *R26R-EYFP* knock-in alleles were maintained in double homozygosity in a mixed genetic background, a condition that did not show any obvious adverse phenotype. To generate experimental litters, males of the double-homozygous stock were mated with CD1 outbred females, so that all embryos from these crosses were double-heterozygous for the inducer and reporter alleles. To induce recombination, pregnant females from timed matings were injected intraperitoneally with 4-hydroxy-tamoxifen (4OHTM) dissolved in corn oil at 0.5 mg/ml. *lacZ* staining [i.e. staining for β-galactosidase (β-gal) activity] was performed as previously described (Torres, 1998). Embryos were post-fixed in 4% paraformaldehyde (PFA) and stored in 80% glycerol, 4% PFA.

Immunohistochemistry

Immunofluorescence for simultaneous detection of Lmx1b and GFP

Embryos were fixed for 30 minutes in 4% PFA, immersed in 30% sucrose until equilibrated, and frozen in OCT embedding compound. Sections (10 μm) were cut, air dried for at least 1 hour and washed twice for 5 minutes each in PBS containing 0.1% Tween 20 (PBT), once for 15 minutes in 0.1% Triton X-100 in PBT and a further twice for 5 minutes each in PBT. Sections were blocked in 5% donkey serum in PBT for 1 hour, followed by incubation for 1 hour at room temperature with goat anti-Lmx1b antibody (Santa Cruz Biotechnology, sc-21231) diluted 1:100 and anti-GFP antibody (Becton Dickinson, Living Colors, 632460) diluted 1:100 in 5% donkey serum in PBT. Sections were then washed three times for 5 minutes each in PBT and incubated with donkey anti-goat Cy3 and donkey anti-rabbit Alexa-488 secondary antibodies for 30 minutes, washed three times for 5 minutes each in PBT and mounted in Vectashield (Vector Laboratories).

Immunohistochemistry for simultaneous detection of β-gal and Lmx1b

Paraffin sections (8 μm) from whole-mount embryos stained for *lacZ* expression were blocked in 3% H_2O_2 in methanol for 25 minutes and washed in distilled water. Antigen retrieval was performed by a 20-minute incubation in a microwave oven at maximum power in tri-sodium citrate buffer pH 6. Sections were then washed in TBST (TBS plus 0.1% Tween-20) for 5 minutes, blocked in 10% goat serum in TBS (15 mM Tris-ClH, 4.5 mM Tris-Base, 150 mM NaCl, pH 7.6) for 30 minutes and subsequently incubated with anti-Lmx1b antibody diluted 1:20 (Abcam, ab-25504) and a biotinylated goat anti-rabbit secondary antibody. Sections were stained using the Vectastain ABC Peroxidase Staining Kit. A similar procedure was used for the simultaneous detection of β-gal and PECAM, except that it was performed on cryostat sections and the antigen retrieval step was omitted.

Statistical analysis

To calculate the probability of polyclonal specimens, independence of the recombination event was assumed. We therefore estimated the expected frequency of polyclonal specimens affecting adjacent regions by multiplying the observed frequency of positive cells in each region in isolation.

Optical projection tomography (OPT)

OPT was performed essentially as described (Sharpe et al., 2002), but with a reduction in the time of dehydration in methanol and clearing in BABB, because longer exposure causes the *lacZ* stain to fade.

Volume rendering and surface mapping were performed using the Visualization Tool Kit software (http://public.kitware.com/VTK/index.php) and the Edinburgh Mouse Atlas software for three-dimensional data processing.

Characterization of an inducible system for clonal analysis in the mouse

To perform retrospective clonal analyses in mouse embryos, we used a genetic strategy based on the site-specific Cre recombinase (Sauer and Henderson, 1988). Labeled cells are produced by the activity of CreERT2, an inducible recombinase activated by tamoxifen (TM) (Feil et al., 1997). Ubiquitous CreERT2 expression is provided by a knock-in insertion of the CreERT2 cDNA into the 3′ UTR of the RNA polymerase II gene (Guerra et al., 2003), which yields viable homozygotes with no obvious phenotype. Cre-mediated recombination is monitored by expression from either the recombination-activatable *R26R* or *R26R-EYFP* knock-in alleles (Soriano, 1999; Srinivas et al., 2001).

To achieve lineage tracing at clonal resolution, we established the conditions for low frequency recombination, such that when a group of positive cells is detected, the probability of polyclonal origin remains low. We achieved this by titrating the dose of 4OHTM. We established the optimal induction dose as 2.5 μg 4OHTM/g of body weight, which yielded frequencies of *lacZ*-positive limbs of 1-20%.

Calculation of the frequency of polyclonal limbs, however, can only be deduced from the frequency of positive limbs if recombination events behave as independent events; that is, if the occurrence of a recombination event does not correlate with the occurrence of a second one in the surrounding cells. To determine this, we induced recombination in embryos carrying both the *lacZ* and the *EYFP Rosa26* recombination reporters. After inducing recombination, we recorded the frequency of limbs positive for *EYFP*, *lacZ*, or both reporters. The frequencies we obtained were in complete agreement with the occurrence of independent recombination events (Table 1).

Another relevant parameter is whether recombination takes place homogeneously across the limb bud. To study this, we induced recombination at a high 4OHTM dose and analyzed the results 24 hours later, to minimize cell movements that might distort the original

Table 1. Independence of recombination events

Frequency of reporter-positive limbs (n=21)			
lacZ	*EYFP*	Both (observed)	Both (expected)
67.7%	33.3%	19%	22%

recombination map. A homogeneous distribution of positive cells was obtained across the three limb bud axes (see Fig. S1A in the supplementary material).

Background recombination in this system is consistently low, with only two out of 204 limbs showing spontaneous positive cells at E14.5. These two clones were composed of very few cells (see Fig. S1B in the supplementary material; data not shown), indicating a late induction event.

Finally, to establish the effective period of clone induction, we determined clone frequency at different times after 4OHTM injection. At the low 4OHTM dose used, we first detected *lacZ*-positive cells 12 hours after 4OHTM injection at E9.5, but few recombination events were detected at this stage (see Fig. S1C in the supplementary material; Table 2). Most induced clones are already detectable 24 hours after injection, with little increase in clone frequency after this (see Fig. S1D,E in the supplementary material; Table 2). To determine the minimum time of induction, we cultured E9.5 embryos in vitro in a high 4OHTM concentration (50 μM) and found that 6 hours were necessary to observe the first *lacZ*-positive cells (data not shown). We thus estimate that the majority of recombination events take place between 12 and 18 hours after 4OHTM injection.

RESULTS

To perform systematic retrospective clonal analysis in the developing mouse embryo, we established a general method for time- and frequency-controlled induction of random-labeled cells (see Materials and methods for details). The method relies on the use of ubiquitously expressed knock-in alleles and is suitable for non-invasive permanent cell labeling during embryonic development. As confirmation of the suitability of this approach for systematic lineage analysis in the developing mouse embryo, we were able to detect the previously characterized lineage relationships of the D-V compartments of the limb ectoderm (Fig. 1A-C) (Kimmel et al., 2000). In the current study, we have analyzed the topological distribution of cell clones in the limb mesenchyme.

Limb mesenchyme shows D-V compartmentalization

Mice pregnant with embryos at stages E8.5, E9.5 and E10.5 were injected with 4-hydroxy-tamoxifen (TM), and the distribution of induced clones examined between E12.5 and E14.5. Analysis of positive cell distribution within the limb was performed both by direct whole-mount visualization of *lacZ* staining and by optical projection tomography (OPT) (n=37) (Sharpe et al., 2002). At all injection stages, considerable dispersion of positive cells along the P-D and A-P axes was observed, indicating a strong tendency for limb mesenchyme cells to disperse and intermingle with neighbors (Fig. 2A). Considerable cell dispersal was also observed along the D-V axis; however, in most specimens dispersal was restricted to one side of a plane dividing the limb into dorsal and ventral sectors, and this affected dorsal and ventral clones similarly (Fig. 2B-H and Table 3). OPT analysis confirmed that the distribution of cells at the ventral limits of dorsal clones (and vice versa) define D-V planes (Fig. 3).

Table 2. Time dynamics of clone induction

	12 h	24 h	36 h	48 h
Total clones	1	90	92	112
Total limbs	36	18	31	24
Clones/limb	0.03	5	3	4.7

Number of clones versus hours after 4OHTM injection.

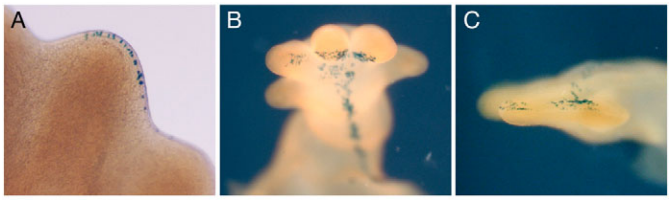

Fig. 1. Clonal analysis identifies previously described compartments and lineage relationships. *lacZ* staining of embryos after 4OHTM injection at E8.5 during gestation. Clone distribution delineates lineage compartmentalization of mouse limb ectoderm into dorsal AER (**A**), ventral ectoderm (**B**) and dorsal ectoderm (**C**).

Apart from restriction at this D-V boundary, pronounced cell dispersal was observed across the dorsal or ventral regions. This apparent freedom of movement, coupled with the consistent and remarkably straight boundary at the D-V mid-plane, shows that the lineage restriction cannot be the result of chance.

To determine whether the frontiers respected by dorsal and ventral clones are consistently located at a reproducible position along the D-V axis, we measured the relative extension of a collection of dorsal and ventral clones at specific positions along the P-D axis of digits 2, 3 and 4 at E13.5 and E14.5. The positions of the boundary measured for each independent dorsal or ventral clone were remarkably consistent, with the majority of boundaries formed at a position displaced dorsally from the midline in 5% of the total D-V extension (Fig. 2I). These results thus identify a single specific boundary at a precise position along the D-V limb axis, which is similarly respected by dorsal and ventral cells.

In a fraction of limbs, however, we detected positive cells, both at dorsal and at ventral positions, that did not respect this boundary (Table 3). A statistical analysis to determine whether these violations might be explained by the presence of multiple clones predicted that 4.0% of E8.5 injections and 4.4% of E9.5 injections would contain independent clones in both dorsal and ventral compartments. However, the observed proportion of limbs showing no D-V restriction was 15% for E8.5 injections and 14% for E9.5 injections. By contrast, at E10.5 we found that the proportion of unrestricted clones was slightly higher but not significantly different from that expected for double recombination events. These results indicate a strong but not complete D-V lineage restriction in early limb bud stages. Full D-V lineage restriction appears to take place only after ~E10.

Vascular cells are insensitive to limb mesenchyme compartmentalization

Limb mesenchyme is composed of resident cells derived from the lateral plate mesoderm and several other incoming cell populations. Our strategy labels not only resident limb mesenchymal cells, but also other cell lineages such as skeletal muscle, endothelium, smooth muscle, melanoblasts and cells of hematopoietic origin. The observed D-V restriction operates on derivatives of resident limb cells, as the vast majority of restricted clones colonized skeletal elements and other derivatives of resident mesenchyme (see below). However, the incoming cell populations that contribute to the limb could not be assessed from the *lacZ* whole-mount stainings alone. An exception to this limitation was the skeletal muscle clones, which could be identified by morphology, were found in a low proportion

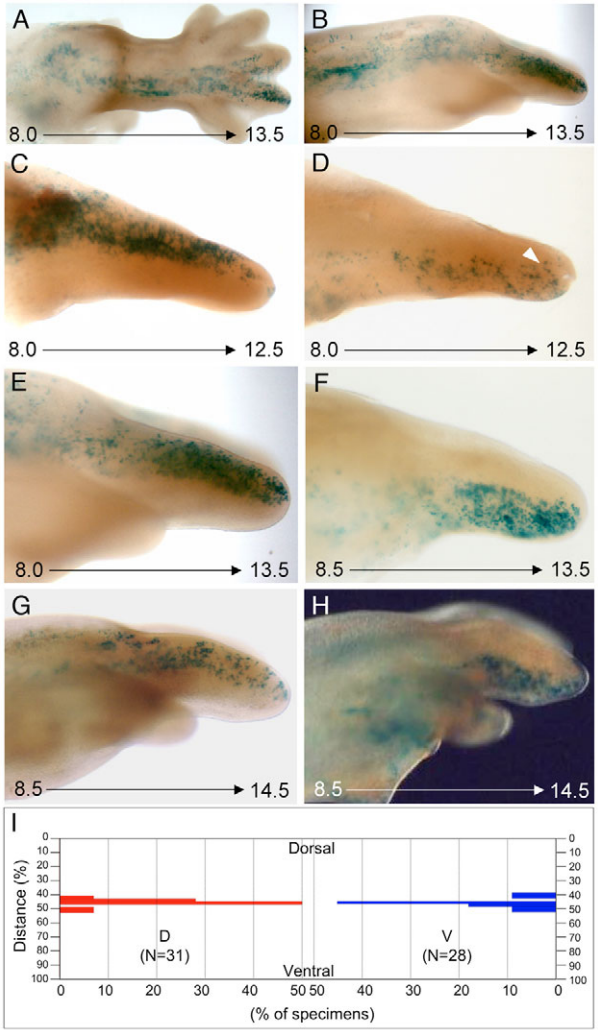

Fig. 2. D-V compartmentalization of limb mesenchyme. (**A-H**) *lacZ* staining of mouse embryos after 4OHTM injection at different gestational stages and recovery at various days of development, as indicated. (A,B) Dorsal and lateral views, respectively, of a large clone induced at E8.0. (C-H) Examples of D-V clone distribution at different embryonic stages, as indicated. The arrowhead in D indicates a local violation of the D-V restriction. (**I**) Bar chart indicating the position of the boundary respected by dorsal (left, red) and ventral (right, blue) clones, expressed as the percentage of the total D-V distance from dorsal. The *x*-axis indicates the percentage of specimens from each class.

of ~1% (3 out of 312) and were found restricted to either dorsal or ventral muscle masses. This observation reflects the independent ingression into the limb of muscle precursors for ventral and dorsal masses (for a review, see Christ and Brand-Saberi, 2002).

We therefore performed an analysis of markers for other incoming cell populations on sections from limbs containing D-V–unrestricted *lacZ*-positive clones. We used PECAM (also known as Pecam1 – Mouse Genome Informatics) to track endothelial lineages and CD45 (also known as Ptprc) to track hematopoietic lineages in 12 specimens containing clones that violated the D-V boundary. In none of these specimens did we find colocalization of CD45 with clone cells; however, we found that in one specimen all clone cells colocalized with PECAM

Table 3. Dorsoventral restriction of mesenchymal clones

Injection day	Total specimens	Positive		Dorsally restricted		Ventrally restricted		Unrestricted	
		n	%	*n*	%	*n*	%	*n*	%
8.5	1820	146	8	74	51	50	34	22 (6)*	15 (4)*
9.5	5640	504	9	247	49	187	37	70 (22)	14 (4.5)
10.5	394	108	27	67	62	29	27	12† (9)	11 (8.4)

*Values in parentheses indicate the number and percentage of cases that can be accounted for by the occurrence of two independent clones in dorsal and ventral compartments.
†One clone identified as endothelial by inspection of whole-mount.

(Fig. 4). *lacZ*-positive cells of this clone had a characteristic appearance and distribution in the whole-mount specimen. This characteristic pattern could easily be identified in other unrestricted clones; we analyzed three of these clones for colocalization with PECAM in sections, and found PECAM-positive clone cells in all three cases (not shown). The ability to identify clones contributing to the vascular network in whole-mounts allowed us to estimate that clones of this class account for ~8% of unrestricted clones (9 out of 109 screened). Unfortunately, we found no histological marker that would allow simultaneous detection of clone cells and melanoblasts, a cell population that colonizes the limb bud by E13.5 (Mackenzie et al., 1997). We were thus unable to determine the contribution of this population to unrestricted clones.

Lmx1b defines the mesenchymal dorsal compartment

Dorsoventral patterning of the vertebrate limb involves the dorsalizing action of the secreted molecule Wnt7a, produced by the dorsal ectoderm (Parr and McMahon, 1995). Countering this, BMP signaling in the ventral ectoderm promotes ventralization by activating the transcription factor En1 (Ahn et al., 2001; Logan et al., 1997; Pizette and Niswander, 2001). In the dorsal mesoderm, the transcription factor Lmx1b (Lmx1 in the chick) responds to Wnt7a signals and specifies the dorsal mesenchymal structures (Chen et al., 1998; Riddle et al., 1995; Vogel et al., 1995).

We noted that the dorsal mesenchymal limb compartment we identified resembles the expression domain of *Lmx1b* (Dreyer et al., 2004; Schweizer et al., 2004). In distal undifferentiated limb regions, the *Lmx1b*-positive dorsal domain is slightly smaller than the *Lmx1b*-negative ventral domain (Fig. 5A,C). At single-cell resolution, the *Lmx1b* expression domain border was not completely straight, showing some interdigitation between *Lmx1b*-positive and *Lmx1b*-negative cells (Fig. 5E,I). To determine the correlation between D-V compartmentalization and *Lmx1b* expression, we double-stained limbs for *Lmx1b* and clone cells, and found that the dorsal-most cells of ventral clones were located next to the ventral-most *Lmx1b*-expressing cells (*n*=5) (Fig. 5F-I). Cells of ventral clones did not express *Lmx1b*, even when surrounded by *Lmx1b*-expressing cells (Fig. 5I). Consistent with the results obtained for ventral clones, ventral-most cells of dorsal clones coincided with ventral-most *Lmx1b*-expressing cells (*n*=6) (Fig. 5D,E; Fig. 6E-J). The *Lmx1b* expression domain thus coincides with the dorsal limb mesenchyme compartment, and *Lmx1b* expression is excluded from the ventral compartment.

In more-proximal limb regions, chondrogenic condensations take place at the boundary between dorsal and ventral cells, as defined by *Lmx1b* expression. Within the early prechondrogenic condensation,

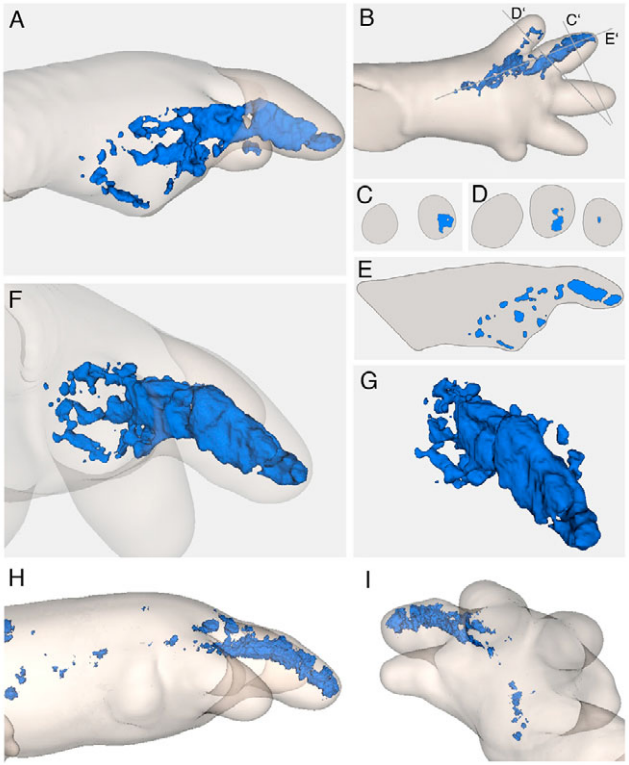

Fig. 3. Optical projection tomography mapping of D-V clone expansion domains. Three-dimensional representations and virtual sections of ventral (**A-G**) and dorsal (**H**,**I**) clones in E14.5 mouse limbs. (A,F) Lateral and oblique views, respectively, of a ventral clone. (B) Ventral view of the same limb. Lines C′-E′ indicate the planes of the virtual sections in C-E, respectively. (G) The three-dimensional clone domain in isolation. (H,I) Lateral and oblique views, respectively, of a dorsal clone.

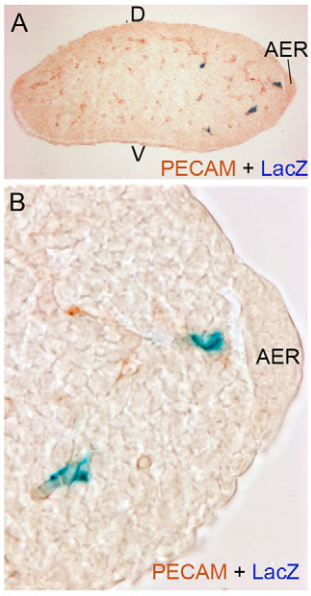

Fig. 4. Vascular endothelial clones do not respect the D-V restriction. (**A**,**B**) Immunohistochemical detection of PECAM (brown) and β-gal (blue) on a cross-section of an E11.5 mouse limb bud. B is an enlargement of the distal portion of the section shown in A.

Lmx1b was expressed in a dorsal domain, showing that chondrogenic cells are recruited from both dorsal and ventral compartments, and therefore that the condensations contain the boundary between dorsal and ventral cells (Fig. 5B; Fig. 6F). As condensations mature, *Lmx1b* expression was lost in the chondrogenic area but remained in the surrounding tissues, maintaining its relative position with respect to the condensation (Fig. 5A; Fig. 6G).

The D-V restriction of the clones affected both the distal undifferentiated limb tissues and the more-proximal differentiating regions. Whereas the D-V frontier was remarkably straight in distal limb regions, it became less uniform in differentiated regions of the limb, suggesting that the frontier between dorsal- and ventral-derived tissues is deformed as they terminally differentiate. In correlation with the *Lmx1b* expression pattern, the D-V compartment boundary appeared to run across the skeletal condensations, dividing them into dorsal and ventral domains (Fig. 5D-G; Fig. 6E-J). In the prechondrogenic condensations, the expression limit of the fading *Lmx1b* expression domain corresponded with the ventral-most location of dorsal clone cells (Fig. 6F,I). In the surrounding differentiating soft tissues the limits of clone expansion also correlated with the position of the frontier within the chondrogenic condensation (Fig. 5F,G; Fig. 6G,J).

There is no compartmentalization along the A-P axis, which is, however, characterized by the temporal and spatial regulation of cell dispersion dynamics

In our analysis, clonal A-P expansion varied according to clone size. Early-induced large clones colonized up to nearly a half of the total A-P axis extension, whereas small clones expanded less widely (Fig. 7A-C, see also Fig. 3A and Fig. 8F). Strikingly, despite extensive mixing of clone cells with their neighbors, most clones displayed straight A-P boundaries running parallel to the main limb axis, so that the fraction of the A-P axis colonized by a given clone remained constant along most of the limb P-D axis. Although this growth pattern suggested possible A-P lineage restrictions, mapping the boundaries for different clones identified no specific frontiers respected by limb cells in their expansion across the A-P axis (not shown).

Clone cell distribution in the autopod showed additional interesting features. We observed two characteristic complementary classes of clones: inter-digital and mid-digital clones (Fig. 7C-F). Inter-digital clone cells were loosely distributed across the whole inter-digital area and the lateral regions of adjacent digits, but stopped abruptly at straight boundaries lateral to the midline of the two neighboring digits. Mid-digital clone cells, conversely, were densely packed and restricted to the central region of a single digit. Mixed clones that partly colonize both areas were also detected and, again, mapping the boundaries for different clones identified no specific respected frontiers. These results indicate there are no A-P compartment restriction boundaries and, in fact, that there is a very notable heterogeneity in cell behavior across the autopod A-P axis. Whereas cells in the inter-digital and lateral digit areas actively disperse and intermingle with neighbors, cells at the central digit regions retain the ordered growth and reduced mixing observed in other P-D limb segments.

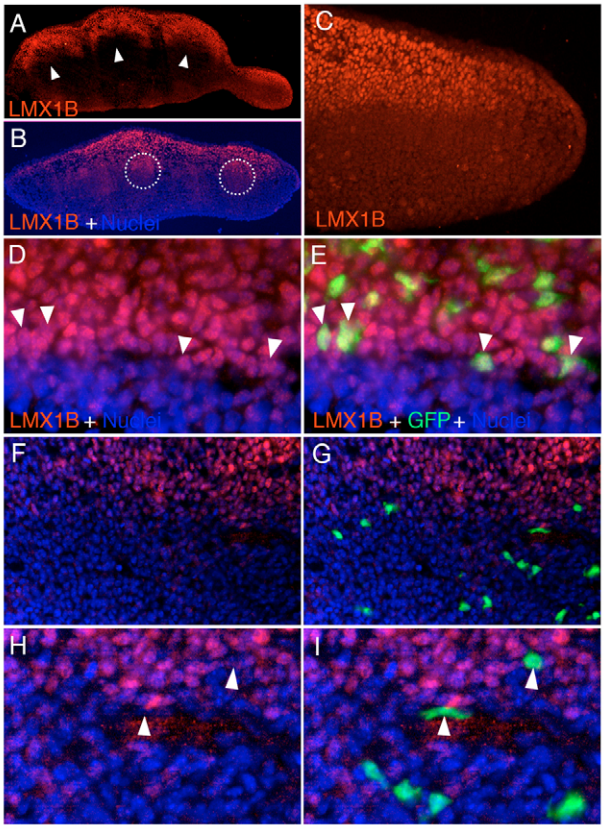

Fig. 5. The D-V lineage restriction boundary correlates with the Lmx1b expression domain. (**A-C**) Immunodetection of Lmx1b protein. (A) An E13.5 autopod sectioned transversally. Arrowheads indicate the sites of chondrogenic condensation. (B) A transversal section of an E13.5 mouse limb at the level of the digital prechondrogenic condensations (circles). (C) A longitudinal section of the undifferentiated digit tip at E13.5. (**D-I**) Immunodetections on E11.5 limbs. (E,G,I) Lmx1b expression, together with the distribution of GFP-positive cells. (D,F,H) The same fields as in E, G and I, respectively, but excluding the GFP channel to reveal Lmx1b expression in clone cells (arowheads). D and E show in detail the distribution of cells belonging to a dorsal clone in relationship to the Lmx1b D-V boundary. Low- (F,G) and high-magnification (H,I) views showing the distribution of cells belonging to a ventral clone in relationship to the Lmx1b D-V boundary.

Limb cells are not allocated by lineage to proximodistal segments in the early limb bud

Vertebrate limbs develop in a proximal-to-distal sequence, being patterned along the three axes by the coordinated action of three signaling centers. One of these centers, the AER, is located at the interface of dorsal and ventral ectoderm. The AER produces signals that maintain a population of distal undifferentiated mesenchymal cells in the underlying region. As the limb bud grows, mesenchymal cells exit the distal region and differentiate to generate limb structures in a proximal-to-distal sequence (Rowe and Fallon, 1982; Saunders, 1948).

We found that clone expansion along the P-D axis was considerable, with a large proportion of clones spanning more than one main limb segment (stylopod, zeugopod, autopod) (Fig. 8A-D). The results obtained were similar for injections at E8.5 and E9.5, and for large clones and small ones, even if composed of very few cells (Fig. 8A-C). Violations of P-D segment frontiers occurred both with clones affecting the skeletal elements and with clones affecting surrounding tissues (Fig. 8D). In view of the frequency of *lacZ* positives for each segment, we estimated the probability of polyclonal origin in cases of multi-segment *lacZ* positives. For this analysis we only considered clones affecting skeletal elements, as these constitute the defining elements for limb P-D specification. We also pooled the data from fore- and hindlimbs, as we observed similar ranges of violation frequencies. In all cases, the observed frequencies of clones violating the frontiers between adjacent P-D segments were incompatible with an independent polyclonal origin ($P<10^{-4}$) (Table 4), indicating that single-cell descendants can indeed contribute to more than one limb segment. When a clone was restricted to one segment, we never observed accumulation of labeled cells at the edges of any given P-D segment (Fig. 8E,F), as sometimes happens at the borders between lineage compartments. We conclude that the main P-D limb segments do not behave as lineage restriction domains at the stages examined. Furthermore, a high proportion of clones (up to 50% for injections at E8.5), besides contributing to differentiating limb regions, included cells in the undifferentiated distal mesenchyme (Table 4). This indicates that cells in this region have a strong tendency to produce descendants that are able both to contribute to the differentiating structures and to remain undifferentiated under the AER.

DISCUSSION

We have presented here the characterization of a general method for clonal analysis in the mouse. The system has the principal characteristics required for an informative clonal analysis: random homogeneous and ubiquitous clone induction, control of induction frequency and timing, low background clone induction, and the possibility of using two independent reporters. The method is validated by its successful detection of previously determined lineage compartments. Given the ubiquitous expression of both the reporter and the inducer transgenes, the system is valid for lineage tracing studies at any stage during embryonic development or adult life, and can be applied to the study of any tissue or organ.

We report the topological distribution of clones induced during limb development. Vertebrate limb development has been extensively used as a suitable model to understand patterning mechanisms (reviewed by Tickle, 2003). Detailed fate maps of the chick limb mesenchyme have been obtained recently by labeling groups of cells with lipophilic dyes (Altabef et al., 1997; Dudley et al., 2002; Saadi et al., 1993; Sato et al., 2007; Vargesson et al., 1997) or by viral infection (Dudley et al., 2002). In the mouse, GIFM of Shh-expressing and Shh signal-receiving cells has been used to determine the fate of ZPA cells (Harfe et al., 2004; Scherz et al., 2004) and of cells receiving Shh signal (Ahn and Joyner, 2004). These approaches have provided important information about limb growth dynamics and have suggested important modifications to established models of limb A-P and P-D patterning; however, they were not done at clonal resolution.

Clonal distribution along the limb A-P axis

We found that early-induced large clones derived from single cells colonize considerable A-P extensions by mixing extensively with neighboring cells. At the same time, these clones have remarkably straight A-P borders, so that their relative contribution to the total A-P limb extension is maintained at constant size and position along the P-D axis. These borders do not represent lineage restrictions, but rather indicate that limb cell precursors keep their relative positions along the A-P axis as they contribute progressively to the P-D axis. These results suggest that during an early phase, cells disperse

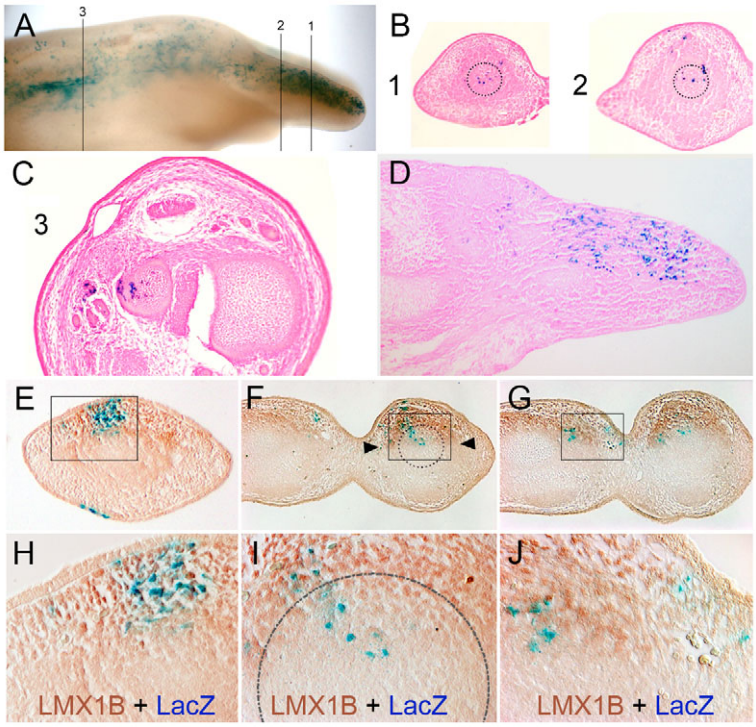

Fig. 6. The D-V restriction boundary runs across the chondrogenic condensations. (**A-D**) Paraffin sections of dorsal clone-containing E14.5 mouse limbs stained for *lacZ* expression. (B,C) Transverse sections of the specimen shown in A at the indicated positions. (**E-J**) Immunohistochemical detection of Lmx1b (brown) and β-gal (blue) on cross-sections of E13.5 digits containing dorsal clones. Circles (B,F,I) indicate the sites of prechondrogenic condensations. Rectangles in E-G indicate the regions shown at higher magnification in H-J. Arrowheads (F) indicate the ventral boundary of Lmx1b expression, which is fading but still visible within the prechondrogenic condensation and coincides with the ventral-most position of *lacZ*-positive cells.

vigorously across the limb primordium, so that descendants of single cells can colonize large sectors of the total initial limb bud. A second phase, likely to start when the limb bud starts to elongate, would be characterized by the cessation of cell mixing and therefore the maintenance of the relative A-P positions of cells in the undifferentiated distal mesenchyme. During autopod generation, ordered growth is maintained at the mid-digital region, while intense cell mixing behavior is regained in the inter-digital areas. Multiple cell-labeling experiments in the chick autopod also suggested extensive mixing in the inter-digital areas versus restricted cell movement in the mid-digital regions (Omi et al., 2000). As a result of this restricted movement, mid-digital areas constitute barriers for the dispersion of inter-digital cells, a phenomenon that might be relevant in the light of the recent model proposing that inter-digital regions are responsible for specifying digit identity (Dahn and Fallon, 2000).

Clonal distribution along the limb P-D axis

Two alternative models have been proposed to explain P-D specification in the limb bud. One model proposes that an autonomous mechanism for progressive distalization is operative in the progress zone (PZ), which is defined as the region of undifferentiated mesenchymal cells under the influence of AER signals (Summerbell et al., 1973). The more recent early allocation model proposes instead that cells in the early limb bud are first simultaneously specified to the main limb P-D segments in the early limb bud and then expand, get irreversibly determined, and differentiate in a proximal-to-distal sequence (Dudley et al., 2002; Sun et al., 2002). The results of our clonal analysis indicate that there are no lineage restrictions at any position along the P-D limb axis at the stages examined. Lineage tracing, however, does not assess cell specification status and therefore does not exclude the existence of a pre-pattern of P-D regional specification in the early limb bud. The results obtained nonetheless argue against a strong formulation of the early allocation model, in which individual cells would be assigned to specific P-D fates early in limb bud development. Similar results have recently been reported in the chick (Pearse et al., 2007; Sato et al., 2007).

D-V compartmentalization of the vertebrate limb mesenchyme

The most significant result from our analysis is the detection of a lineage boundary that subdivides the resident limb mesenchyme into dorsal and ventral compartments. The compartmentalization observed may extend to some incoming cell lineages that enter the limb from external sources, such as the skeletal muscle precursors, whose dorsal mass cells acquire *Lmx1b* expression as they enter the limb (Schweizer et al., 2004), but not to others, such as endothelial cells, which we found to be insensitive to the D-V border. A D-V lineage restriction has also been detected in parallel studies by retroviral clonal analysis in the chick (Pearse et al., 2007) and GIFM from the *Lmx1b* locus in the mouse (R. Johnson, personal communication).

This is the first example in metazoans of a lineage compartment operating in a mesenchymal structure. As such, these compartments are organized in three dimensions and their borders are not lines, as is the case in epithelial compartments, but rather a plane between mesenchymal cells. This finding suggests that compartmentalization strategies during embryonic development might be more widely used than previously thought, especially in vertebrates, in which patterning of three-dimensional mesenchymal structures is a frequent process.

The identification of lineage compartment borders in *Drosophila* was achieved through the use of cell clones that have a growth advantage with respect to the cells of the background [wild-type cells versus *Minute* mutant cells] (Garcia-Bellido et al., 1973). Despite the reduced tendency of imaginal disc cells to disperse, this growth advantage allowed wild-type clones to colonize enough territory to delineate the compartment borders, demonstrating the robustness of the mechanisms restricting cell mixing between compartments. In the case of the vertebrate limb, the mesenchymal

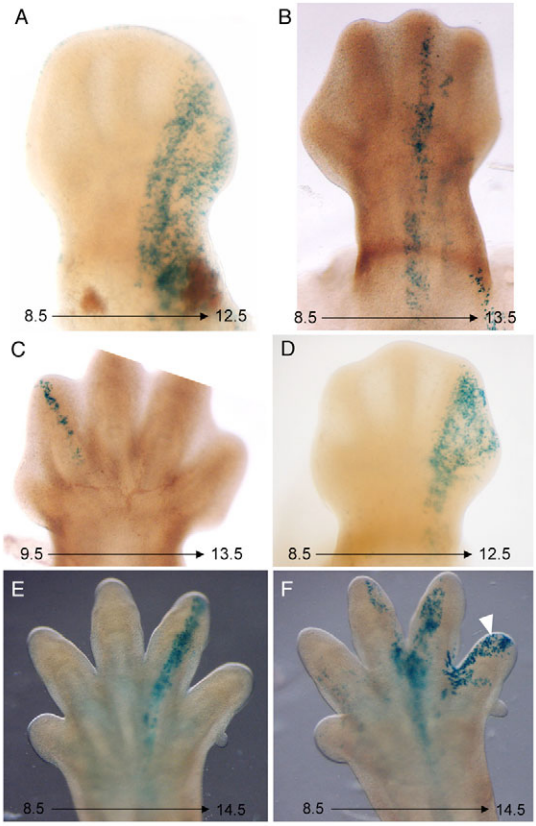

Fig. 7. Clone distribution along the A-P axis. (**A-F**) *lacZ* staining of mouse embryos after 4OHTM injection at different stages during gestation and recovery on different days of development, as indicated. The arrowhead (F) indicates *lacZ*-positive cells of an independent ectodermal clone.

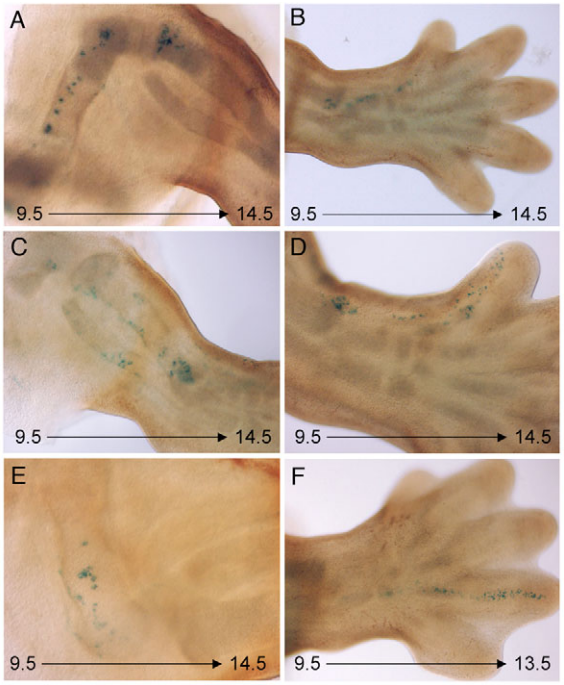

Fig. 8. Clone distribution indicates no compartmentalization along the P-D axis. (**A-F**) *lacZ* staining of mouse embryos after 4OHTM injection at different stages during gestation and recovery on different days of development, as indicated. (A,C) Examples of violation of the stylopod-zeugopod frontier. (B,D) Examples of violation of the zeugopod-autopod frontier. (E,F) Examples of clones respecting the frontiers.

cells exhibit a strong tendency to disperse during organ growth, resulting in the occupation of large volumes by clones composed of a relatively small number of cells, such that the compartment border is effectively delineated by the majority of the clones in the absence of any growth advantage. It remains to be explored, however, whether the restriction mechanisms operating in the vertebrate limb mesenchyme are sufficiently robust to avoid cell mixing in the case of clones that do have a growth advantage.

One of the most notable characteristics of the vertebrate limb D-V compartmentalization is that it subdivides the primordium into parts that do not correspond to or anticipate any anatomical or cell-type interface. They might thus be different from compartments described so far in vertebrates, which do correlate with transient or definitive anatomical frontiers. The vertebrate limb D-V subdivision therefore appears to result from a background modular design of the developmental field, unrelated to the need to sort cells destined for different anatomical elements or that belong to diverse histotypes. In this sense, the compartments described here might be more similar to classical *Drosophila* compartments than to others previously described in vertebrates.

Genetic regulation of vertebrate limb compartmentalization

Compartments are independent patterning units that express specific selector genes essential for maintaining compartment-specific properties and for regulating pattern formation within their territory (Morata and Lawrence, 1975). We found that the territory corresponding to the limb dorsal compartment correlates with the expression domain of the transcription factor Lmx1b. Eliminating *Lmx1b* function in the mouse results in double-ventral limbs (Chen et al., 1998), and overexpression of the ortholog gene *Lmx1* in chicken results in double-dorsal limbs (Riddle et al., 1995; Vogel et al., 1995), demonstrating this factor's essential role in dorsal specification. Qiu and co-workers (R. Johnson, personal communication) report that at least some of the cellular properties involved in maintaining the dorsal compartment are encoded by *Lmx1b* and that after an initial unstable period, *Lmx1b* expression is transmitted stably to daughter cells. This is supported by results with chicken explants and recombinant limbs, which suggest that after an initial phase of activation by Wnt7a, *Lmx1* expression is stably maintained independently of external cues (Piedra et al., 2000; Riddle et al., 1995). However, expression of *Lmx1b* is not dorsally restricted in the early mouse limb bud (Loomis et al., 1998), a result which suggests that the mesenchymal D-V compartment might not be established in the early limb bud and might appear only after *Lmx1b* expression becomes restricted to dorsal regions. In fact, our results suggest that D-V restriction is incomplete in 4OHTM injections at or before E9.5. Previous studies in the chick failed to identify any D-V lineage restriction in limb mesenchyme before HH16 (Altabef et al., 1997), indicating that compartmentalization in the chick may take place after this stage and after the initial *Lmx1* activation at stage HH15+ (Altabef and Tickle, 2002). Indeed, the

Table 4. Clone contribution to proximodistal segments

	Positives						Violations		
Injection day	Total limbs	Total limbs	Stylopod (S)	Zeugopod (Z)	Autopod (A)	DM*	S-Z	Z-A	S-Z-A
8.5	360	24	7	16	14	12	5 (0.8)†	8 (0.9)	3 (0.06)
9.5	524	63	24	33	28	18	8 (1.6)	12 (1.9)	2 (0.08)

*Distal, undifferentiated mesenchyme.
†Values in parentheses indicate the number of limbs expected to contain two independent clones in the adjacent P-D segments.

initial D-V specification of limb mesoderm depends on external signals, first from paraxial mesoderm and lateral somatopleura, and later from ectoderm (Michaud et al., 1997).

Similar to classical compartments in *Drosophila* and others described later in vertebrates, the dorsal limb mesenchymal compartment therefore appears to constitute an independent unit of genetic regulation, and *Lmx1b* appears to be a major regulator of its properties.

Besides the *Lmx1b* expression transition, there was no other feature that we could associate with the mesenchymal D-V boundary, even at electron microscope resolution (data not shown). A barrier mechanism for the maintenance of the lineage restriction border is therefore unlikely. The compartment boundary might instead be maintained by a differential adhesion mechanism that restricts the strong tendency of mesenchymal limb cells to disperse and mix with neighbors. Such a mechanism would fit well with the observed irregular shape of the border between *Lmx1b*-positive and *Lmx1b*-negative cells.

Functional significance of limb mesenchyme D-V compartmentalization

One of the most widely accepted ideas about compartments is that lineage restriction serves to stabilize signaling centers at compartment borders, which constitute organizers for adjacent compartments (reviewed by Vincent, 1998). Classical insect compartment borders, as well as the AER and the MHB in vertebrates, are signaling centers with organizer properties. Compartments at both sides of these borders are independent developmental fields that respond to the organizer activity of the signaling center. Lineage boundaries with no organizer activity, such as rhombomeric limits, also express signaling molecules with essential patterning functions. By contrast, in the case of the D-V limb mesenchymal border, there is no evidence for any organizer or specific signaling activity, as none of the known signaling molecules is specifically expressed at the D-V interface. The subdivision of the developmental field into independent units of patterning and growth might thus be a more fundamental characteristic of lineage compartments than their association with signaling regions. In the case of mesenchymal compartments, in addition to defining independent patterning units, compartmentalization might be relevant to the complex morphogenetic movements that three-dimensional mesenchymal structures such as limb buds have to go through (for example, D-V flattening and bending). Exploring the existence of further compartments of this sort will determine how widely this mechanism is used to pattern mesenchymal fields during metazoan development.

We thank Mariano Barbacid, Mª Victoria Campuzano and Carmen Guerra for the *RERT* mice, Shankar Srinivas for the *R26R-EYFP* mice, Jesús García-Herrero for advice on the statistical calculations, Estefanía Escudero for mouse colony management, Cristina Herranz for excellent technical assistance and Cristina Clavería for advice on antibody stainings. We are grateful to Alfonso Martínez-Arias, Peter Lawrence, Jose Luis de la Pompa, Marian Ros and Juan José Sanz-Ezquerro for helpful advice on manuscript preparation. We thank Simon Bartlett for editorial corrections to the manuscript. C.G.A. was supported by a fellowship from the Ministerio de Educación y Ciencia. This work was supported by grants from the Spanish Ministerio de Educación y Ciencia (BFU2006-10978/BMC), the Human Frontiers Science Program (RGP0008/2004) and the European Commission (LSHG-CT-2003-5032259). CNIC is supported by the Spanish Ministry of Health and Consumer Affairs and the Pro-CNIC Foundation.

Supplementary material

Supplementary material for this article is available at
http://dev.biologists.org/cgi/content/full/134/20/3713/DC1

References

Ahn, K., Mishina, Y., Hanks, M. C., Behringer, R. R. and Crenshaw, E. B., 3rd (2001). BMPR-IA signaling is required for the formation of the apical ectodermal ridge and dorsal-ventral patterning of the limb. *Development* **128**, 4449-4461.
Ahn, S. and Joyner, A. L. (2004). Dynamic changes in the response of cells to positive hedgehog signaling during mouse limb patterning. *Cell* **118**, 505-516.
Altabef, M. and Tickle, C. (2002). Initiation of dorso-ventral axis during chick limb development. *Mech. Dev.* **116**, 19-27.
Altabef, M., Clarke, J. D. and Tickle, C. (1997). Dorso-ventral ectodermal compartments and origin of apical ectodermal ridge in developing chick limb. *Development* **124**, 4547-4556.
Blair, S. S. (2003). Lineage compartments in Drosophila. *Curr. Biol.* **13**, R548-R551.
Bonnerot, C. and Nicolas, J. F. (1993). Clonal analysis in the intact mouse embryo by intragenic homologous recombination. *C. R. Acad. Sci. III* **316**, 1207-1217.
Brocard, J., Warot, X., Wendling, O., Messaddeq, N., Vonesch, J. L., Chambon, P. and Metzger, D. (1997). Spatio-temporally controlled site-specific somatic mutagenesis in the mouse. *Proc. Natl. Acad. Sci. USA* **94**, 14559-14563.
Chen, H., Lun, Y., Ovchinnikov, D., Kokubo, H., Oberg, K. C., Pepicelli, C. V., Gan, L., Lee, B. and Johnson, R. L. (1998). Limb and kidney defects in Lmx1b mutant mice suggest an involvement of LMX1B in human nail patella syndrome. *Nat. Genet.* **19**, 51-55.
Christ, B. and Brand-Saberi, B. (2002). Limb muscle development. *Int. J. Dev. Biol.* **46**, 905-914.
Dahn, R. D. and Fallon, J. F. (2000). Interdigital regulation of digit identity and homeotic transformation by modulated BMP signaling. *Science* **289**, 438-441.
Dreyer, S. D., Naruse, T., Morello, R., Zabel, B., Winterpacht, A., Johnson, R. L., Lee, B. and Oberg, K. C. (2004). Lmx1b expression during joint and tendon formation: localization and evaluation of potential downstream targets. *Gene Expr. Patterns* **4**, 397-405.
Dudley, A. T., Ros, M. A. and Tabin, C. J. (2002). A re-examination of proximodistal patterning during vertebrate limb development. *Nature* **418**, 539-544.
Feil, R., Wagner, J., Metzger, D. and Chambon, P. (1997). Regulation of Cre recombinase activity by mutated estrogen receptor ligand-binding domains. *Biochem. Biophys. Res. Commun.* **237**, 752-757.
Fraser, S., Keynes, R. and Lumsden, A. (1990). Segmentation in the chick embryo hindbrain is defined by cell lineage restrictions. *Nature* **344**, 431-435.
Garcia-Bellido, A., Ripoll, P. and Morata, G. (1973). Developmental compartmentalisation of the wing disk of Drosophila. *Nat. New Biol.* **245**, 251-253.
Guerra, C., Mijimolle, N., Dhawahir, A., Dubus, P., Barradas, M., Serrano, M., Campuzano, V. and Barbacid, M. (2003). Tumor induction by an endogenous K-ras oncogene is highly dependent on cellular context. *Cancer Cell* **4**, 111-120.
Harfe, B. D., Scherz, P. J., Nissim, S., Tian, H., McMahon, A. P. and Tabin, C. J. (2004). Evidence for an expansion-based temporal Shh gradient in specifying vertebrate digit identities. *Cell* **118**, 517-528.
Joyner, A. L. and Zervas, M. (2006). Genetic inducible fate mapping in mouse: Establishing genetic lineages and defining genetic neuroanatomy in the nervous system. *Dev. Dyn.* **235**, 2376-2385.
Kiecker, C. and Lumsden, A. (2005). Compartments and their boundaries in vertebrate brain development. *Nat. Rev. Neurosci.* **6**, 553-564.
Kimmel, R. A., Turnbull, D. H., Blanquet, V., Wurst, W., Loomis, C. A. and Joyner, A. L. (2000). Two lineage boundaries coordinate vertebrate apical ectodermal ridge formation. *Genes Dev.* **14**, 1377-1389.

Lawrence, P. A. (1973). A clonal analysis of segment development in Oncopeltus (Hemiptera). *J. Embryol. Exp. Morphol.* **30**, 681-699.
Legue, E. and Nicolas, J. F. (2005). Hair follicle renewal: organization of stem cells in the matrix and the role of stereotyped lineages and behaviors. *Development* **132**, 4143-4154.
Logan, C., Hornbruch, A., Campbell, I. and Lumsden, A. (1997). The role of Engrailed in establishing the dorsoventral axis of the chick limb. *Development* **124**, 2317-2324.
Loomis, C. A., Kimmel, R. A., Tong, C. X., Michaud, J. and Joyner, A. L. (1998). Analysis of the genetic pathway leading to formation of ectopic apical ectodermal ridges in mouse Engrailed-1 mutant limbs. *Development* **125**, 1137-1148.
Mackenzie, M. A., Jordan, S. A., Budd, P. S. and Jackson, I. J. (1997). Activation of the receptor tyrosine kinase Kit is required for the proliferation of melanoblasts in the mouse embryo. *Dev. Biol.* **192**, 99-107.
Mathis, L. and Nicolas, J. F. (2000). Different clonal dispersion in the rostral and caudal mouse central nervous system. *Development* **127**, 1277-1290.
Mathis, L., Sieur, J., Voiculescu, O., Charnay, P. and Nicolas, J. F. (1999). Successive patterns of clonal cell dispersion in relation to neuromeric subdivision in the mouse neuroepithelium. *Development* **126**, 4095-4106.
Meilhac, S. M., Kelly, R. G., Rocancourt, D., Eloy-Trinquet, S., Nicolas, J. F. and Buckingham, M. E. (2003). A retrospective clonal analysis of the myocardium reveals two phases of clonal growth in the developing mouse heart. *Development* **130**, 3877-3889.
Meilhac, S. M., Esner, M., Kelly, R. G., Nicolas, J. F. and Buckingham, M. E. (2004). The clonal origin of myocardial cells in different regions of the embryonic mouse heart. *Dev. Cell* **6**, 685-698.
Michaud, J. L., Lapointe, F. and Le Douarin, N. M. (1997). The dorsoventral polarity of the presumptive limb is determined by signals produced by the somites and by the lateral somatopleure. *Development* **124**, 1453-1463.
Morata, G. and Lawrence, P. A. (1975). Control of compartment development by the engrailed gene in Drosophila. *Nature* **255**, 614-617.
Nicolas, J. F., Mathis, L., Bonnerot, C. and Saurin, W. (1996). Evidence in the mouse for self-renewing stem cells in the formation of a segmented longitudinal structure, the myotome. *Development* **122**, 2933-2946.
Omi, M., Sato-Maeda, M. and Ide, H. (2000). Role of chondrogenic tissue in programmed cell death and BMP expression in chick limb buds. *Int. J. Dev. Biol.* **44**, 381-388.
Parr, B. A. and McMahon, A. P. (1995). Dorsalizing signal Wnt-7a required for normal polarity of D-V and A-P axes of mouse limb. *Nature* **374**, 350-353.
Pearse, R. V., II, Scherz, P. J., Campbell, J. K. and Tabin, C. J. (2007). A cellular lineage analysis of the chick limb bud. *Dev. Biol.* (in press).
Piedra, M., Rivero, F., Fernandez-Teran, M. and Ros, M. A. (2000). Pattern formation and regulation of gene expressions in chick recombinant limbs. *Mech. Dev.* **90**, 167-179.
Pizette, S. and Niswander, L. (2001). Early steps in limb patterning and chondrogenesis. *Novartis Found. Symp.* **232**, 23-36; discussion 36-46.
Riddle, R. D., Ensini, M., Nelson, C., Tsuchida, T., Jessell, T. M. and Tabin, C. (1995). Induction of the LIM homeobox gene Lmx1 by WNT7a establishes dorsoventral pattern in the vertebrate limb. *Cell* **83**, 631-640.
Rowe, D. A. and Fallon, J. F. (1982). The proximodistal determination of skeletal parts in the developing chick leg. *J. Embryol. Exp. Morphol.* **68**, 1-7.
Saadi, A., Gallien, C. L., Guyot-Lenfant, M. and Chanoine, C. (1993). A new approach of urodele amphibian limb regeneration: study of myosin isoforms and their control by thyroid hormone. *Mech. Dev.* **43**, 49-56.
Sato, K., Koizumi, Y., Takahashi, M., Kuroiwa, A. and Tamura, K. (2007). Specification of cell fate along the proximal-distal axis in the developing chick limb bud. *Development* **134**, 1397-1406.
Sauer, B. and Henderson, N. (1988). Site-specific DNA recombination in mammalian cells by the Cre recombinase of bacteriophage P1. *Proc. Natl. Acad. Sci. USA* **85**, 5166-5170.
Saunders, J. W. (1948). The proximodistal sequence of origin of the parts of the chick wing and the role of the ectoderm. *J. Exp. Zool.* **108**, 363-403.
Scherz, P. J., Harfe, B. D., McMahon, A. P. and Tabin, C. J. (2004). The limb bud Shh-Fgf feedback loop is terminated by expansion of former ZPA cells. *Science* **305**, 396-399.
Schweizer, H., Johnson, R. L. and Brand-Saberi, B. (2004). Characterization of migration behavior of myogenic precursor cells in the limb bud with respect to Lmx1b expression. *Anat. Embryol.* **208**, 7-18.
Sharpe, J., Ahlgren, U., Perry, P., Hill, B., Ross, A., Hecksher-Sorensen, J., Baldock, R. and Davidson, D. (2002). Optical projection tomography as a tool for 3D microscopy and gene expression studies. *Science* **296**, 541-545.
Soriano, P. (1999). Generalized lacZ expression with the ROSA26 Cre reporter strain. *Nat. Genet.* **21**, 70-71.
Srinivas, S., Watanabe, T., Lin, C. S., William, C. M., Tanabe, Y., Jessell, T. M. and Costantini, F. (2001). Cre reporter strains produced by targeted insertion of EYFP and ECFP into the ROSA26 locus. *BMC Dev. Biol.* **1**, 4.
Summerbell, D., Lewis, J. and Wolpert, L. (1973). Positional information in chick limb morphogenesis. *Nature* **224**, 492-496.
Sun, X., Mariani, F. V. and Martin, G. R. (2002). Functions of FGF signalling from the apical ectodermal ridge in limb development. *Nature* **418**, 501-508.
Tickle, C. (2003). Patterning systems – from one end of the limb to the other. *Dev. Cell* **4**, 449-458.
Torres, M. (1998). The use of embryonic stem cells for the genetic manipulation of the mouse. *Curr. Top. Dev. Biol.* **36**, 99-114.
Vargesson, N., Clarke, J. D., Vincent, K., Coles, C., Wolpert, L. and Tickle, C. (1997). Cell fate in the chick limb bud and relationship to gene expression. *Development* **124**, 1909-1918.
Vincent, J. P. (1998). Compartment boundaries: where, why and how? *Int. J. Dev. Biol.* **42**, 311-315.
Vogel, A., Rodriguez, C., Warnken, W. and Izpisua Belmonte, J. C. (1995). Dorsal cell fate specified by chick Lmx1 during vertebrate limb development. *Nature* **378**, 716-720.
Wilkie, A. L., Jordan, S. A., Sharpe, J. A., Price, D. J. and Jackson, I. J. (2004). Widespread tangential dispersion and extensive cell death during early neurogenesis in the mouse neocortex. *Dev. Biol.* **267**, 109-118.